JOURNAL OF Materials CHEMISTRY

Synthesis and characterization of $MgO–B_2O_3$ mixed oxides prepared by coprecipitation; selective dehydrogenation of propan-2-ol

M. A. Aramendía, V. Boráu, C. Jiménez, J. M. Marinas, A. Porras and F. J. Urbano*

Department of Organic Chemistry, Faculty of Sciences, University of Córdoba, Avda. San Alberto Magno s/n, E-14004 Córdoba, Spain. E-mail: qo1urnaf@uco.es

Received 28th September 1998, Accepted 27th November 1998

The synthesis of $MgO–B_2O_3$ mixed oxides by coprecipitation from $Mg(OH)_2$ and $B(OH)_3$ (0–10 wt%) led to solids with textural and acid–base properties rather different from pure magnesium oxide. DRIFT and ^{11}B MAS NMR studies showed that boron atoms are in a flat trigonal environment, as part of the magnesium oxide structure. Titration of acid and basic sites by TPD–MS of probe molecules (pyridine and 2,6-dimethylpyridine for acid sites, and carbon dioxide for basic ones) indicates that the presence of boron leads to an increase in the acid sites surface density as well as to a decrease in surface density of basic ones, together with a change in strength distribution profile of the later. Propan-2-ol conversion over $MgO–B_2O_3$ mixed oxides showed an increase in the selectivity to the dehydrogenation process with an increase in the amount of boron in the catalyst.

Introduction

Magnesia is considered, together with CaO and BaO, as a typical basic oxide (Hammett constant $H_- = +26.0$).[1–4] This solid can be obtained by thermal treatment of the hydroxide or carbonate, or by the so-called 'sol–gel method'. Textural and acid–base properties depend, to a great extent, on the synthesis conditions (pH, gelifying agent, sequence of addition of reagents, calcination temperature, *etc.*).[5–7]

The basic sites in magnesium oxide are due to the presence of low coordination surface oxygen anions (O^{2-}). Such anions are located in corners, edges, *etc.*, and are responsible for basic sites of different strength. By contrast, acid sites are related to electron-deficient surface magnesium atoms (Mg^{+2}).[8–12] The modification of such acid–base properties is usually carried out by mixing MgO with other oxides,[13] metallic ions[14–17] or noble metals,[18] and is a very effective way of tailoring the activity towards many organic processes.

Boron oxide is one of additives widely used to modify textural and acid–base properties of metal oxides such Al_2O_3[19–21] and TiO_2,[22] leading, in general, to an increase in the number of acid sites together with a decrease in that of basic ones. The preparation procedure of such mixed oxides can be either by coprecipitation or impregnation, the former leading to higher acidity.[23] $Al_2O_3–B_2O_3$ mixed oxides are very suitable for many organic reactions such as but-2-ene selective synthesis from ethanol,[24] or the Beckmann rearrangement,[25] and are more resistent to deactivation by coking.

However, the preparation of $MgO–B_2O_3$ mixed oxides, as yet, has not been thoroughly studied. Ueshima and Shimasaki[26] have shown that the addition of small amounts of boron oxide (<1%) resulted in an increase in acidity (Hammett constant between +7.0 and +12.0). Those modifications change the catalytic behaviour of the solids towards some organic reactions, such as the improvement of the selectivity to unsaturated alcohols in the gas-phase hydrogen-transfer reduction of α,β-unsaturated carbonyl compounds.

This work deals with the preparation of $MgO–B_2O_3$ mixed oxides from coprecipitation of $Mg(OH)_2$ and $B(OH)_3$ [0–10 wt% $B(OH)_3$]. Textural characterization of the resulting solids has been carried out from adsorption–desorption isotherms of nitrogen, XRD, DRIFT and ^{11}B MAS NMR. Acid-base properties have been obtained from temperature-programmed desorption experiments with detection by mass spectrometry (TPD-MS), of probe molecules (pyridine, 2,6-dimethylpyridine for acid sites and carbon dioxide for basic ones) following a precedure described elsewhere.[27,28]

The solids prepared have been tested in the dehydration–dehydrogenation of propan-2-ol, widely used to correlate the catalytic activity with the surface acid–base properties.[29–31]

Experimental

Catalyst synthesis

The mixed oxides ($MgO–B_2O_3$) were prepared from magnesium hydroxide [$Mg(OH)_2$, Merck Art. 5827] and boric acid (H_3BO_3 Sigma Art. B-7660), by the coprecipitation method. An aqueous $Mg(OH)_2$ solution is acidified with concentrated nitric acid and the required amount of boron was added from an aqueous solution of $B(OH)_3$. To this continuously stirred mixture was added a solution of 3 M NaOH from a Braun perfusor at a rate of 300 mL min^{-1} until a white solid was obtained (pH = 10). The gel obtained was held at room temperature for 24 h and then filtered, thoroughly washed and dried in an oven at 120 °C for 24 h. The dried solid was crushed and calcined in flowing air (40 mL min^{-1}) in a quartz reactor from room temperature up to 600 °C at a rate of 6 °C min^{-1}. The final temperature was held for 3 h and the solid was then cooled in flowing air. The nomenclature used for the mixed oxides is MgB-*x*, where *x* is the wt% of boric acid in the initial mixture (0, 1, 5 or 10%).

Thermal analysis of the precursors

Thermal analysis of the precursors was performed on a Micromeritics temperature programmed desorption-temperature programmed reaction instrument (TPD/TPR 2900) that was fitted to a VG Sensorlab quadrupole mass spectrometer from Fisons Instruments plc/VG quadrupoles (East Sussex, UK) operating in the multiple ion monitoring (MIM) mode. An amount (*ca.* 40 mg) of precursor was placed in the middle of the reactor (1 cm id, 20 cm long) and flowing nitrogen (50 mL min^{-1}) was set at room temperature for 15 min. Then, the temperature was raised to 600 °C at a rate of 5 °C min^{-1}.

Adsorption isotherms and surface area

The textural properties of the solids (specific surface area, pore volume and mean radius) were determined from nitrogen adsorption–desorption isotherms at liquid nitrogen temperature by using a Micromeritics ASAP-2000 instrument. Surface

areas were calculated by the BET method[32] while pore distributions were determined by the BJH method[33] (adsorption branch, cylindrical pores open on one side only and adsorbed layer thickness calculated by the Halsey method). All samples were degassed at 350 °C to 0.1 Pa prior to measurement.

X-Ray diffraction and ^{11}B MAS NMR spectra

X-Ray diffraction patterns for the solids were recorded on a Siemens D-500 diffractometer equipped with an automatic control and data acquisition system (DACO-MP). Patterns were run from nickel-filtered copper radiation ($\lambda = 1.5405$ Å) at 35 kV and 20 mA, the diffraction angle 2θ being scanned at 2° min^{-1}.

Room temperature ^{11}B MAS NMR measurements were carried out on a Bruker ACP 400 spectrometer. Samples were heated in a nitrogen flow (50 mL min^{-1}) for 4 h at 150 °C, then cooled down in an N_2 flow and transferred to the sample holder in an environmental chamber (in nitrogen atmosphere). Spectra were acquired with a 90° pulse (0.4 μs) and the repetition time was 2 s. The rotation frequency was 5.5 kHz. The chemical shifts were expressed relative to $BF_3 \cdot Et_2O$.

Diffuse reflectance IR spectroscopic experiments

DRIFT experiments were conducted on a Bomen MB-100 instrument with an 'Environmental Chamber' from Spectra-Tech. The instrument was operated at a resolution of 8 cm^{-1} over the range 4000–400 cm^{-1} to gather 256 scans.

Temperature-programmed desorption–mass spectrometry (TPD–MS) experiments

TPD–MS experiments were carried out on the above described Micromeritics TPD/TPR 2900—VG Sensorlab quadrupole mass spectrometer. The optimum TPD conditions were as follows: heating rate 10 °C min^{-1} and an Ar flow-rate of 50 mL min^{-1}. The mass spectrometer, which was operated in the MIM mode, was programmed to perform 6 scans min^{-1}.

The amines used as probe molecules in order to determine the acid properties of the solids were pyridine (p$K = 5.25$) and 2,6-dimethylpyridine (p$K = 7.3$). In a previous diffuse reflectance IR (DRIFT) study of the bands for the two amines in the region 1400–1700 cm^{-1}, Marinas and coworkers[34] found pyridine to be adsorbed at Brönsted and Lewis acid sites, and 2,6-dimethylpyridine to be adsorbed on the former site type only owing to the steric hindrance of its two methyl substituents. The peaks used to quantify pyridine were the base peak (m/z 79) and the secondary peak at m/z 52 (80% abundance). The MS peaks chosen for 2,6-dimethylpyridine were the base peak (m/z 107) and the secondary peak at m/z 66 (60% abundance). Calibration was done by injecting pulses of variable size (1–10 μL) of a 10^{-5}–10^{-6} M amine solution in cyclohexane.

Carbon dioxide was the probe molecule used to determine the basic properties of the catalysts. The gases used in the CO_2 TPD–MS experiments, CO_2 and 5% CO_2 in argon, were both supplied by Sociedad Española de Oxígeno S.A (>99.999%). Carbon dioxide was quantified by its base (m/z 44) and secondary peaks (m/z 12, 10% abundance). Calibration was performed by injecting variably size pulses of pure CO_2 or 5% CO_2 in Ar. Several replicates of each experiment provided a mean error of 2% in peak areas.

Prior to adsorption of any probe molecule, each catalyst was cleaned by passing an Ar stream at 110 °C at 50 mL min^{-1} for 30 min. The solids were then saturated by passing an amine–N_2 or CO_2–Ar stream (50 mL min^{-1}) at 25 and 50 °C, respectively. Subsequently, a pure N_2 or Ar stream (50 mL min^{-1}) was passed at the saturation temperature for 2 h in order to remove any physisorbed molecules. Once a stable baseline was obtained, chemisorbed amine or CO_2 was desorbed by heating from saturation temperature to 600 °C in a programmed fashion. The selected mass peaks were monitored throughout the process. Each experiment used *ca.* 100 mg of fresh catalyst. Full details of the TPD–MS method and equipment are given elsewhere.[27,28]

Propan-2-ol conversion

Propan-2-ol test reaction was carried out in a pulse microreactor fitted to a gas chromatograph HP Mod. 5890 equipped with a semicapillary column Supelcowax-10 (30 m, id = 0.53 mm). The pulse size was 0.5 μL and the carrier gas was nitrogen at a rate of 75 mL min^{-1}. The reaction temperatures varied from 300 to 400 °C with a stabilization time for each temperature of 15 minutes. The weight of catalyst used in each experiment was 20–30 mg. Prior to the reaction, several experiments were carried out to ensure that the reaction is under kinetic control. The absence of any diffusional effect was verified in each case.

Results and discussion

Thermal analysis of the precursors

The thermal analysis of both isolated precursors [$Mg(OH)_2$ and $B(OH)_3$] is presented in Fig. 1 (profiles a and b) together with the profile corresponding to the solid MgB-5 (profile c). The comparison between the profiles corresponding to magnesium hydroxide and MgB-5 indicates that the temperature of transformation of magnesium hydroxide is not modified by the gel formation proccess in which 5 wt% boric acid is added. This seems to indicate that low percentages of boric acid do not significantly alter the structure of the magnesium oxide, the boron atoms are considered located in a trigonal or tetragonal environment within the magnesium network. As we see later, XRD and ^{11}B MAS NMR studies give more information on this matter. Moreover, Mazza *et al.*,[35] from crystallographic studies of Al_2O_3–B_2O_3 mixed systems, proposed theoretical models in wich the mullite Al_2O_3 structure does not suffer any alteration when boron atoms are located within the net structure.

Adsorption isotherms and surface area

All nitrogen adsorption–desorption isotherms corresponding to the catalysts MgB-x were classified as type IV in the

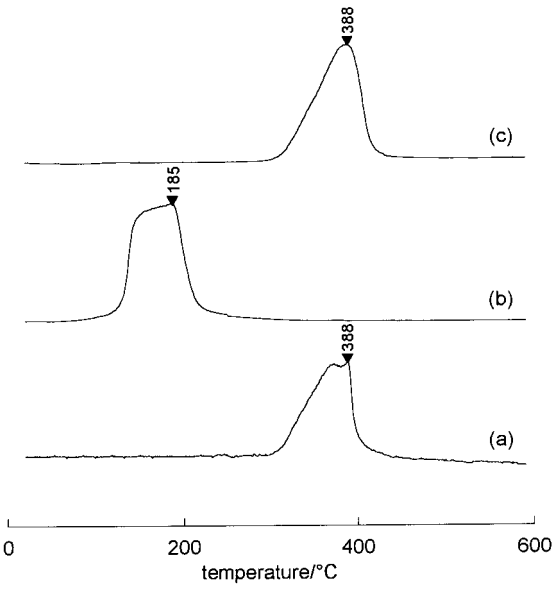

Fig. 1 Thermal analysis of the precursors of MgB-5 catalyst: (a) $Mg(OH)_2$, (b) H_3BO_3, (c) gel corresponding to the MgB-5 catalyst.

Table 1 Textural properties of the MgB-x catalysts: specific surface area, S_{BET}, mean pore volume, V_p and mean pore radius, r_p

Catalyst	B/Mg	$S_{BET}/m^2\ g^{-1}$	$V_p/cm^3\ g^{-1}$	r_p/Å
MgB-0	0	63	0.33	213
MgB-1	0.01	45	0.26	198
MgB-5	0.04	32	0.15	176
MgB-10	0.10	18	0.05	119

Brunauer, Emmett and Teller classification,[32] associated to mesoporous solids. Table 1 shows the specific surface area (S_{BET}), pore volume (V_P) and mean pore radius (r_P) obtained from such isotherms. The most important feature in this table is that the surface area decreases as the amount of boric acid increases in the final solid ($63\ m^2\ g^{-1}$ for the MgB-0 and $18\ m^2\ g^{-1}$ for the MgB-10). There is also a substantial loss of pore volume.

X-Ray diffraction

Fig. 2 shows the X-ray diffraction patterns for the solids studied in this work. They are similar and exhibit three characteristic peaks for periclase variety of MgO at $d=2.44$, 2.11 and 1.49 nm ($2\theta=36.7$, 42.8 and 62.2°, respectively).[5] Curtin *et al.*[25] describe the appearance of bands corresponding to B_2O_3 in mixed systems at $2\theta=14.2$ and 27.6. Those bands are absent in our systems, leading to the conclusion that the structure of our solids is a periclase MgO network with boron atoms forming part of the structure in a trigonal or tetragonal environment. Similar models were proposed by other authors for mixed systems in wich boron oxide is not the main component, such as Al_2O_3–B_2O_3[20,24,35] and TiO_2–B_2O_3.[22]

Diffuse reflectance IR spectroscopic experiments (DRIFT)

Fig. 3 shows the DRIFT profiles obtained for the solids studied in this work. Such profiles present bands in two spectral regions, between 4000 and 3000 cm^{-1} as well as below

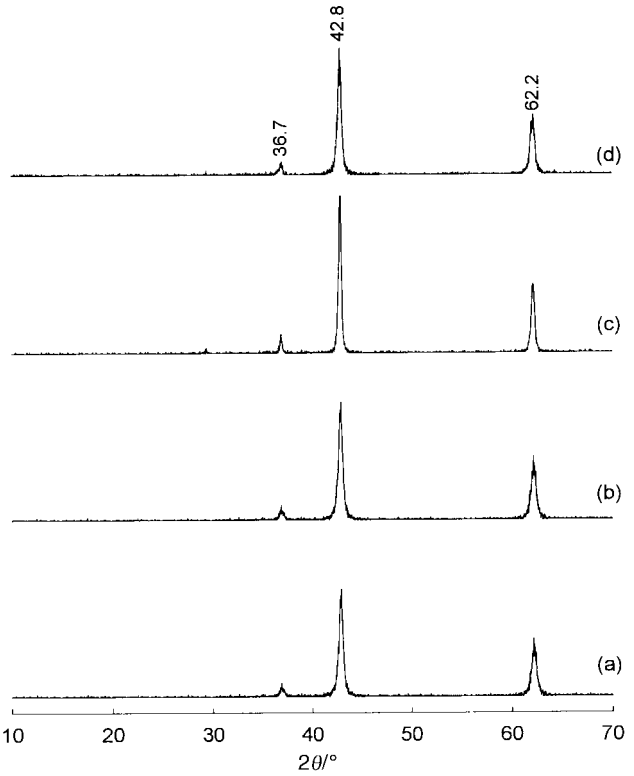

Fig. 2 XRD of the MgB-x catalysts: (a) MgB-0, (b) MgB-1, (c) MgB-5, (d) MgB-10.

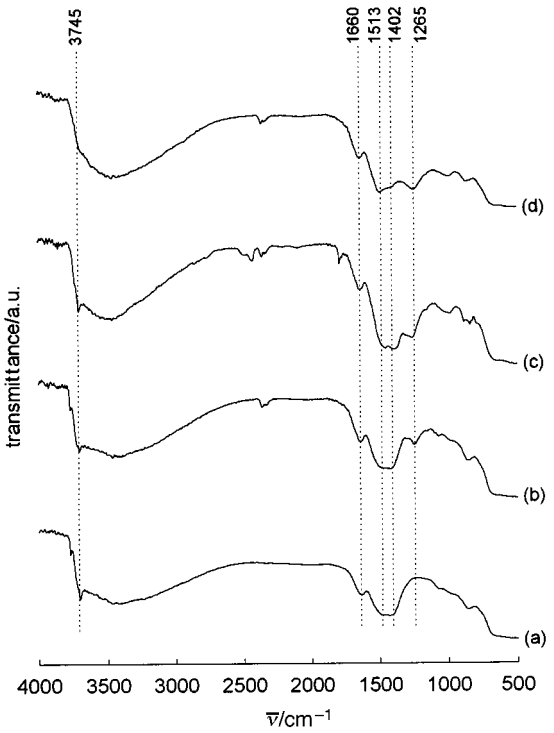

Fig. 3 DRIFT of the MgB-x catalysts: (a) MgB-0, (b) MgB-1, (c) MgB-5, (d) MgB-10.

2000 cm^{-1}. The bands appearing between 4000 and 3000 cm^{-1} are associated with hydroxy group stretching. Kirlin *et al.*[36] established the existence of eight different bands in this region, due to different kinds of OH groups found on the magnesium oxide surface. López *et al.*[5] assigned the narrow band at 3745 cm^{-1} to OH groups not forming hydrogen bonds. They proved that even after calcination at temperatures above 900 °C some hydroxy groups from $Mg(OH)_2$ are still present. The broad band between 3640 and 3500 cm^{-1}, is assigned to OH groups forming weak hydrogen bonds, in a previous state of dehydration.

As far as the region below 2000 cm^{-1} is concerned, two type of bands can be distinguished; those appearing in all solids and those present only in boron containing systems. Thus the 1700–1400 cm^{-1} region includes bands corresponding to O–H and Mg–O stretching,[37–38] that appear in all four catalysts. Moreover, all systems present a broad band below 1000 cm^{-1}, assigned to Mg–O bending. However, the band at 1256 cm^{-1} appears only in boron containing systems. Mazza *et al.*[35] studied the active bands in Raman and IR spectroscopy corresponding to borate ions in trigonal and tetragonal environments. As far as the IR absorption is concerned, the borate ions in trigonal environment present three bands, the most important appearing at around 1300 cm^{-1}, assigned to B–O asymmetric stretching, and present if the borate has calcite type structure disappearing when the structure is aragonite. By contrast tetragonal borate species give two active bands in the IR in the spectral region 1200–1100 cm^{-1}. According to Ramirez *et al.*,[19] all those bands suffer a shift to lower frequencies when boron atoms are neighbours of other atoms in mixed systems (aluminium, titanium, silicon, *etc.*).

Bearing in mind the above comments, it can be concluded that the IR band at 1265 cm^{-1} could be assigned to B–O assymetric stretching of boron atoms in a trigonal environment, shifted to lower frequencies by the neighbouring magnesium atoms (1300 cm^{-1} for isolated trigonal borate ions).

^{11}B MAS NMR

^{11}B MAS NMR spectra of MgB-x mixed oxides (Fig. 4) allow confirmation of the coordination of boron atoms (trigonal or

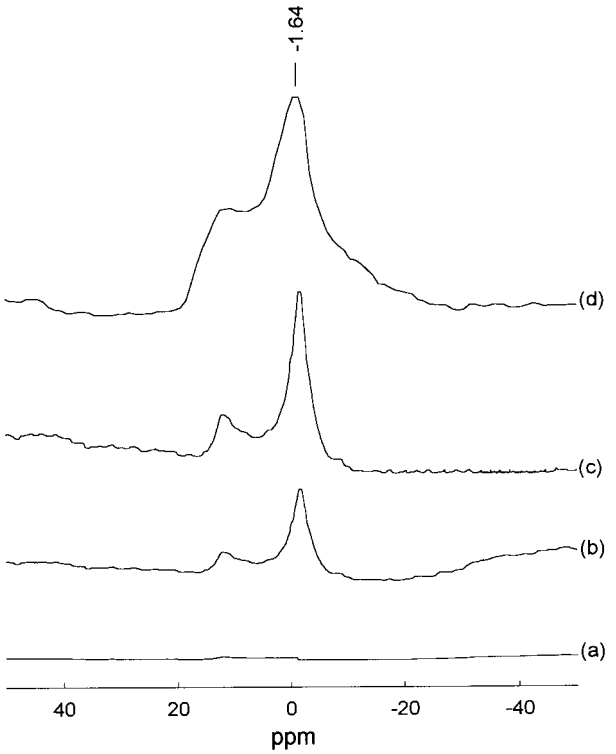

Fig. 4 ^{11}B MAS NMR of the MgB-*x* catalysts: (a) MgB-0, (b) MgB-1, (c) MgB-5, (d) MgB-10.

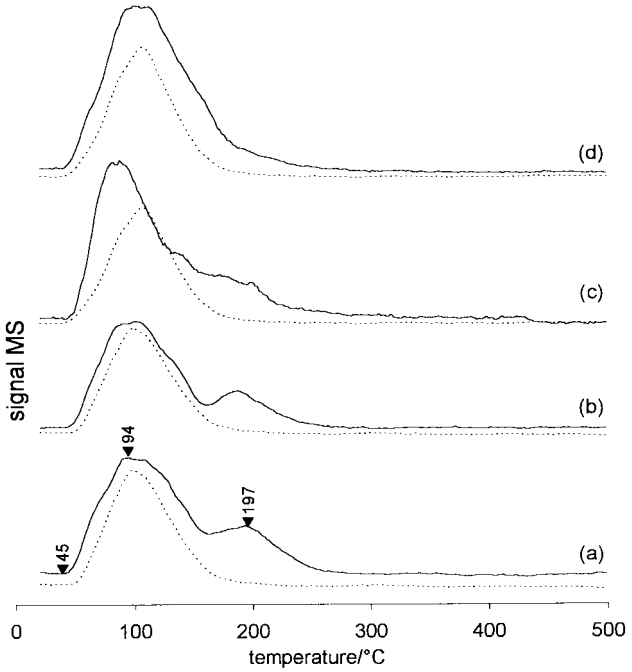

Fig. 5 PY (continuous line) and DMPY (discontinuous line) TPD–MS profiles of the MgB-*x* catalysts: (a) MgB-0, (b) MgB-1, (c) MgB-5, (d) MgB-10.

tetragonal) in our catalysts. Peil *et al.*[39] established that for tetragonal borate species the spectra obtained are rather symmetrical. By contrast, for a trigonal environment, a broad band including a doublet is obtained. The asymmetric spectra corresponding to our solids (Fig. 4) indicate clearly that boron atoms are located in the magnesium network in a trigonal environment, in agreement with the conclusions obtained from DRIFT experiments.

Temperature-programmed desorption–mass spectrometry (TPD–MS) experiments

The characterization of solids catalyst from probe molecules TPD–MS experiments allows us to determine not only the number of active sites but also their strength. Thus the probe molecules used were pyridine (PY) to measure the total (Brönsted and Lewis) acidity, 2,6-dimethylpyridine (DMPY) to determine Brönsted acidity and carbon dioxide to obtain total basicity.

Fig. 5 presents the PY and DMPY TPD-MS profiles while Fig. 6 shows the CO_2 TPD–MS profiles obtained for the MgB-*x* mixed systems. Table 2 collects the numeric values of Bronsted and Lewis acidity and basicity arising from such experiments. In general, as the amount of boron increases the acid sites density notably increases while the basic sites density shows a small decrease. Colorio *et al.*,[20] working with mixed oxides, being B_2O_3 minority (Al_2O_3–B_2O_3, LiO_2–B_2O_3, *etc.*), found similar variation in acid–base properties of such systems.

As far as the acid sites are concerned, the surface density of acid sites in MgB-10 is four times higher than in MgB-0. Moreover the ratio Lewis/Brönsted acid sites increases as with increased boron content, going from 14% in MgB-0 to 26% in MgB-10 (Table 2). On the other hand, a redistribution of acid strength occurs, since the strength of Lewis acid sites decreases with increasing amount of boron in the catalyst, as indicated by the shift to lower temperatures of the PY desorption peak, corresponding to Lewis sites (those appearing at 197 °C in MgB-0 solid, Fig. 5). Therefore, the overall effect is an increase of acidity, mainly in Lewis acid sites, although of lower strength.

Table 2 Acid–base titration of the MgB-*x* catalysts by TPD-MS of preadsorbed probe molecules (PY for total acidity, DMPY for Brönsted acidity and CO_2 for total basicity). r_t = basicity/acidity

	Acid sites density		Basic sites density	
Catalyst	PY/μmol m^{-2}	Lewis (%)	PY/μmol m^{-2}	CO_2/r_t
MgB-0	0.5	14	4.7	8.7
MgB-1	0.7	15	4.6	6.9
MgB-5	1.1	22	4.4	4.0
MgB-10	2.0	26	4.2	2.1

The modification of the basic properties as the amount of boron increases can be seen from two different viewpoints. First, from Table 2 it is clear that basicity suffers a slight but significant decrease on passing from MgB-0 to MgB-10. On the other hand, the strength distribution clearly changes as the boron content increases (Fig. 6). Thus, MgB-0 exhibits three different kind of basic sites whose desorption maxima are at 208, 341 and 577 °C. These peaks become less clear until an single, rather broad peak appearing in MgB-10 solid (apex at 298 °C). As results, a decrease in the basic strength of the basic sites is detected as the boron content increases.

The overall change in acid–base properties as the amount of boron increases can be visualized by the factor r_t, the ratio between basic and acid sites density. Thus, while the MgB-0 (non-boron containing solid) is a mainly basic catalyst (r_t = 8.7) the MgB-10, although still basic, has more equilibrated acid and basic properties (r_t = 2.1). This is crucial for some organic reactions that require pairs of acid–base sites to occur, such as cyclohexane dehydrogenation, *n*-hexane cyclization[22] or the selective synthesis of but-2-ene from ethanol.[24]

Those results allow us, by changing the amount of boron on the catalyst, to prepare the optimum catalyst, as far as the textural and acid–base properties is concerned, for a given organic reaction.[22]

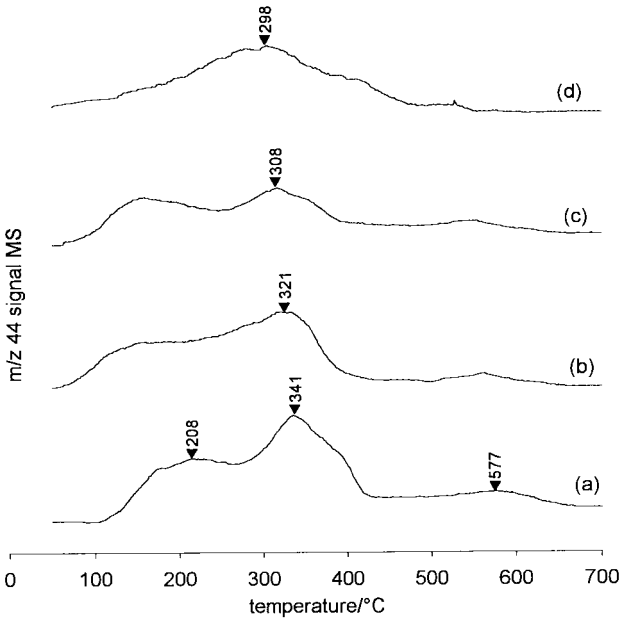

Fig. 6 CO_2 TPD-MS profiles of the MgB-x catalysts: (a) MgB-0, (b) MgB-1, (c) MgB-5, (d) MgB-10.

Propan-2-ol transformation over MgB-x mixed oxides

Both dehydrogenation and dehydration of the alcohol were found to follow first-order kinetic behaviour as described by the Basset–Habgood equation,[40]

$$\ln [1/(1-x)] = kK(W/F)RT$$

where k (s^{-1}) is the kinetic constant, K is the adsorption constant on the catalyst surface (mol atm^{-1} g^{-1}), W is the catalyst weight (g), F is the reactant flow-rate (mL s^{-1}), and x is the conversion [(mol%)/100]. This equation allowed us to obtain the product kK (the so-called pseudo-kinetic constant) for both processes (dehydration and dehydrogenation), at each temperature tested. The activation energies (E_a) and pre-exponential factor (ln A) were derived from the Arrhenius equation.

Table 3 shows the overall conversion X, pseudo-kinetic constants kK and specific pseudokinetic constants kK_{esp} for the propan-2-ol transformation process over the MgB-x mixed oxides at a reaction temperature of 350 °C.

It is clear from Table 3 that the catalytic activity decreases as the amount of boron increases in the solid. However, since the specific surface area also decreases with the boron content, the more appropriate parameter to compare activities is the specific pseudo-kinetic constant (kK_{esp}) in which the decrease in surface area is compensated for.

Propan-2-ol reacts to give acetone and propene and no diisopropyl ether was detected in any experiment. Fig. 7 shows how the overall pseudokinetic constant and selectivity to the dehydrogenation [defined as $S_{acetone} = (X_{acetone}/X_{total}) \times 100$] change with the reaction temperature. The most important feature is the increase in the selectivity to dehydrogenation as the amount of boron increases in the catalysts. The reaction

Table 3 Propan-2-ol conversion over MgB-x catalysts at 350 °C (X, molar conversion; kK, pseudo-kinetic constant, kK_{esp}, specific pseudo-kinetic constant)

Catalyst	B/Mg	X(%)	10^5 kK/ mol atm^{-1} g^{-1} s^{-1}	10^6 kK_{esp}/ mol atm^{-1} s^{-1} m^2
MgB-0	0	9.4	11.6	213.7
MgB-1	0.01	6.3	6.6	198.4
MgB-5	0.04	2.9	3.4	176.7
MgB-10	0.10	1.5	1.8	119.5

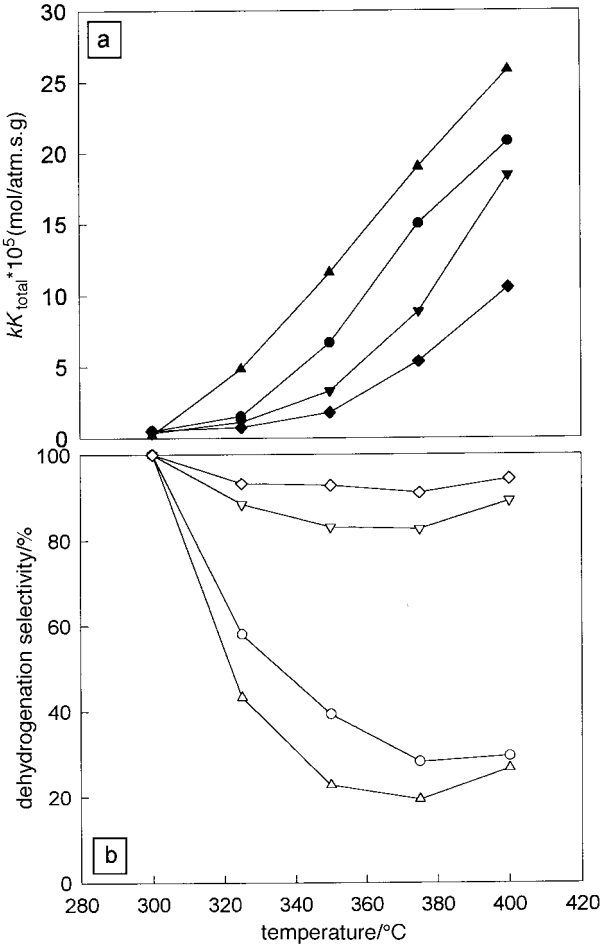

Fig. 7 Overall pseudokinetic constant (a) and selectivity to the dehydrogenation (b) on the propan-2-ol conversion over the MgB-x catalysts: (▲) MgB-0, (●) MgB-1, (▼) MgB-5, (◆) MgB-10.

mechanism would give us valuable information on this change of selectivity. From a general point of view, three different elimination mechanisms can be proposed, E1, E1cB and E2. E1 is a mechanism that takes place by steps on acid solids leading exclusively to dehydration (propene). The E1cB mechanism occurs on basic solids and accounts for both dehydration and dehydrogenation processes. Finally, the E2 mechanism is a concerted process that takes place on amphoteric solids, those having similar number of acidic and basic sites, and accounts for the dehydration process.[41,42] In previous work, a detailed study of those mechanisms was carried out on different oxides.[7] Following this work, the reaction mechanism that takes place on our mainly basic solids would be E1cB. Fig. 8 shows the reaction mechanism proposed leading to dehydrogenation and dehydration. The first step is the interaction of the alcohol with a basic site (O^{2-}), together with the loss of a proton, either from the ß-carbon by forming an adsorbed carbanion **1** or from the hydroxy group by forming an adsorbed alkoxide **2**. The second step would lead to a negatively charged species as a leaving group. Following the adsorbed species **1**, the leaving group would be OH^-, leading to propene (dehydration), while from **2** the leaving group would be H^- from the carbon attached to the hydroxy group, leading to acetone (dehydrogenation). In this sense, Tamaru and other workers[43,44] proved that, working with deuterated propan-2-ol, the preceding step to the formation of acetone is the abstraction of hydride ion. Therefore, the selectivity of the propan-2-ol process over MgB-x mixed systems depends on the relative populations of the intermediate adsorbed species (**1** or **2**) formed on the catalytic surface. If the main species formed is **1**, the process would lead to dehydration whereas if

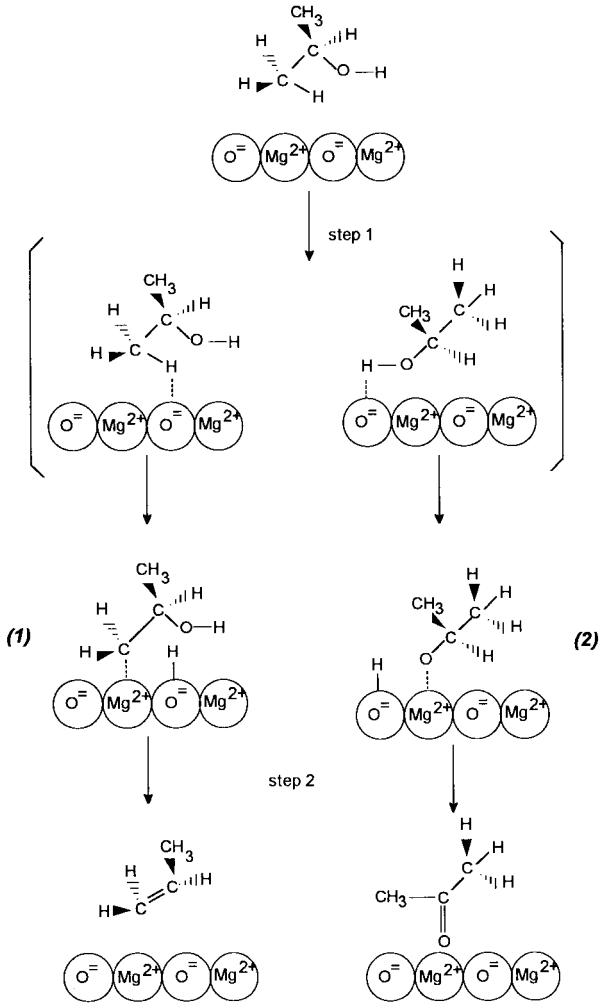

Fig. 8 Propan-2-ol conversion following an E1cB mechanism for the dehydration (a) and dehydrogenation (b) processes.

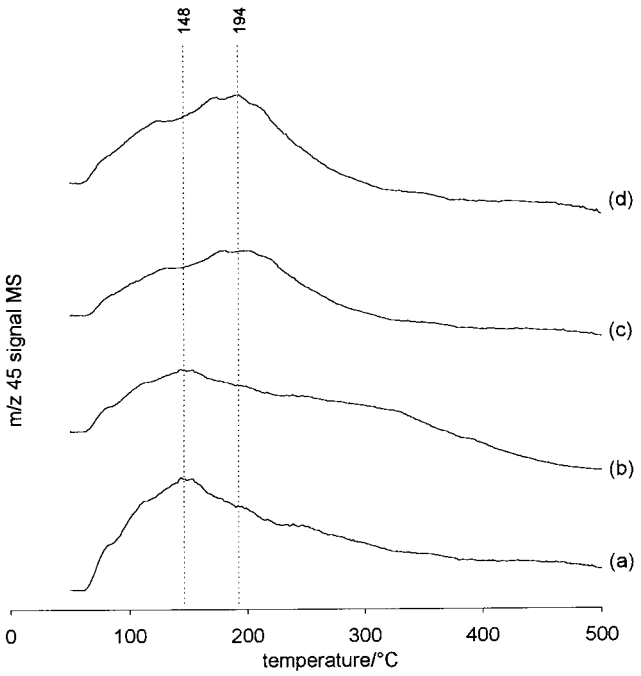

Fig. 9 TPD–MS profiles corresponding to propan-2-ol desorption over the MgB-*x* catalysts: (a) MgB-0, (b) MgB-1, (c) MgB-5, (d) MgB-10.

Table 4 Activation parametres (preexponential factor, ln A and activation energy, E_a) in propan-2-ol conversion (dehydration–dehydrogenation competitive process) over MgB-*x* catalysts

	Dehydration		Dehydrogenation	
Catalyst	ln A	E_a/kJ mol^{-1}	ln A	E_a/kJ mol^{-1}
MgB-0	7.0	86.1	13.0	121.7
MgB-1	8.6	114.2	8.7	100.7
MgB-5	10.2	117.1	7.5	94.6
MgB-10	16.6	140.1	5.1	82.0

the species formed is **2**, the dehydrogenation product would be obtained. Since the alcoholic hydrogen of propan-2-ol is more acidic than those of methyl, the step corresponding to the proton abstraction to form species **1** or **2** would depend on the strength of the catalytic basic sites. Over strong basic sites both types of protons can be abstracted out leading to both species in Fig. 8 and therefore both dehydration and dehydrogenation processes would take place to a similar extent. On the other hand, only the more acidic proton (the alcoholic one) would be abstracted by weak basic sites, leading to the dehydrogenation product with high selectivity. Following this, the increase in the dehydrogenation selectivity in our MgB-*x* catalysts with the boron loading is in accord with the decrease in the strength of the basic sites of those solids.

Experiments involving the adsorption of propan-2-ol on the catalyst surface and its subsequent desorption (TPD–MS profiles) can help to determine the mechanism for the competitive dehydration and dehydrogenation processes. Fig. 9 shows the TPD–MS profiles for propan-2-ol preadsorbed on the MgB-*x* catalysts. One must bear in mind that the alkoxide form **2** which leads to the dehydrogenation product interacts more strongly with the catalyst surface than does the carbanionic form **1** which yields the dehydration product because the O–Mg interaction is stronger than the C–Mg. Therefore, when the TPD for previously adsorbed propan-2-ol is recorded, form **2** will be desorbed at higher temperatures than **1**. This is clearly reflected in the profiles of Fig. 9 from solid MgB–0 (no boron) to MgB-10 (10% boron in the synthetic procedure) and confirms that the adsorption of propan-2-ol on the catalyst surface changes from **1** to **2**.

Application of the Arrhenius equation to the kinetic data of Fig. 7 allows the pre-exponential factor and activation energy for the two competing processes (dehydration and dehydrogenation) on each catalyst to be calculated (see Table 4). Interestingly, the activation energy for the dehydration process increases along the catalyst sequence whereas that for the dehydrogenation process exhibits the opposite trend. If the rate-determining step in the transformation of propan-2-ol on the solids *via* an E1cB mechanism is assumed to be the uptake of a proton to form an adsorbed species (Fig. 8), then this will differ for the two processes, with that giving the lower activation energy being more favoured. As noted earlier, the presence of boron in the MgB-*x* catalysts decreases the activation energy for the dehydrogenation; consequently, this process will be favoured over dehydration.

Conclusions

Doping magnesium oxides with boron (by using magnesium hydroxide and boric acid as precursors) introduces a very interesting change in the textural and acid–base properties of MgO. In principle, increasing amounts of boron decrease the specific surface area of the resulting solid, which is about 30% in MgB-10; in any case, all the solids can be classified as mesoporous. Consequently, an excess of boron atoms dramati-

cally reduces the specific surface area of the solid and hinders its use as a catalyst for organic processes.

The use of physical techniques such as DRIFT and ^{11}B MAS NMR to examine the catalyst revealed boron to lie in a planar trigonal environment and to be a part of the magnesium oxide network (essentially in the periclase variety), as reflected in the XRD patterns for the solids.

As regards acid–base properties, increasing the number of boron atoms considerably increases the density of acid (essentially Lewis) sites and slightly decreases that of basic sites; these effects are accompanied by a decrease in strength in both types of sites. In this respect, it is worth noting the increase (12%) in the number of Lewis acid sites from MgB-10 to MgB-0, even if it is accompanied by a decrease in their strength. The above-mentioned changes in the surface chemical properties result in a change in r_t (*viz.* the ratio of basic to acid site density) from 8.7 in MgB-0 to 2.1 in MgB-10, which is especially interesting for some reactions that require the joint action of acid and basic sites.

The selectivity of the competitive dehydration–dehydrogenation of propan-2-ol depends strongly on the boron content in the solid. Thus, while solid MgB-0 exhibits similar selectivity towards both processes, dehydrogenation is favoured as the boron content is raised. The root of this change in the previous trend is the decreased strength of the basic sites, which favours dehydrogenation in the E1cB mechanism (typical of essentially basic catalysts such as magnesium oxides).

Acknowledgements

We wish to acknowledge funding of this research by Spain's DGES (Project PB97/0446) and by the Consejería de Educación y Ciencia of the Andalusian Regional Government. A. Porras also wishes to acknowledge award of a post-Doctoral fellowship by Fundación Caja de Madrid. Finally, we wish to thank the staff at the Mass Spectrometry and Magnetic Nuclear Resonance services of the University of Córdoba for recording the mass and ^{11}B MAS NMR spectra.

References

1 K. Tanabe, M. Misoko, Y. Ono and H. Hattori, *Stud. Surf. Sci. Catal.*, 1989, **51**.
2 A. Gervasini and A. Auroux, *J. Catal.*, 1991, **131**, 190.
3 R. Sokoll and H. Hobert, *J. Catal.*, 1992, **134**, 409.
4 K. Doll, M. Dolg and H. Stoll, *Phys. Rev. B*, 1996, **54**, 13529.
5 T. Lopez, I. García-Cruz and R. Gomez, *J. Catal.*, 1991, **127**, 75.
6 M. A. Aramendía, V. Boráu, C. Jiménez, J. M. Marinas, A. Porras and F. J. Urbano, *J. Mater. Chem.*, 1996, **6**, 1943.
7 M. A. Aramendía, V. Boráu, C. Jiménez, J. M. Marinas, A. Porras and F. J. Urbano, *J. Catal.*, 1996, **161**, 829.
8 V. R. Choudhary and M. Y. Pandit, *Appl. Catal.*, 1991, **71**, 265.
9 X. D. Peng and M. A. Barteau, *Langmuir*, 1991, **7**, 1426.
10 T. Ito, M. Kuramato, M. Yoshida and T. Tokuda, *J. Phys. Chem.*, 1983, **87**, 4411.
11 T. Ito, T. Murakami and T. Tokuda, *J. Chem. Soc., Faraday Trans.*, 1983, **79**, 913.
12 K. J. Borve and L. G. M. Pettersson, *J. Phys. Chem.*, 1991, **95**, 7401.
13 A. M. Yousssef, L. B. Khalil and B.S. Girgis, *Appl. Catal.*, 1992, **81**, 1.
14 G. Connell and J. A. Dumesic, *J. Catal.*, 1987, **105**, 285.
15 T. Matsuda, Y. Sasaki, H. Miura and K. Sugiyama, *Bull. Chem. Soc. Jpn.*, 1985, **58**, 58.
16 C. R. A. Catlow, L. Ackermann, R. G. Bell, D. H. Gay, S. Hot. D. W. Lewis, M. A. Nygren, G. Sastre, D. C. Sayle and P. E. Sinclair, *J. Mol. Catal.*, 1997, **115**, 431.
17 T. Kanno and M. Kobayashi, *J. Mater. Sci. Lett*., 1997, **16**, 126.
18 E. G. Derouane, V. Jullien-Lardot, R. J. Davis, N. Blom and P. E. Hojlund-Nielsen, *Proceedings of 10th International Congress on Catalysis*, ed. L. Guczi, F. Solymosi and P. Tetenyi, Budapest, Hungary, 1992, p. 1031.
19 J. Ramirez, P. Castillo, L. Cedeño, R. Cuevas, M. Castillo, J. M. Palacios and A. Lopez-Agudo, *Appl. Catal. A*, 1995, **132**, 317.
20 G. Colorio, J. C. Vedrine, A. Auroux and B. Bonnetot, *Appl. Catal. A*, 1996, **137**, 55.
21 G. C. Colorio, A. Auroux and B. Bonnetot, *J. Therm. Anal.*, 1993, **40**, 1267.
22 J. Fung and I. Wang, *J. Catal.*, 1996, **164**, 166.
23 C. Li and Y-W. Chen, *Catal. Lett.*, 1993, **19**, 99.
24 B-Q. Xu, T-X. Cai, J-H. Yu, F-S. Xiao, R-R. Xu, J-S. Huang and Y-D. Xu, *J. Chem. Soc., Chem. Commun.*, 1992, 1228.
25 T. Curtin, J. B. McMonagle and B. K. Hodnett, *Appl. Catal. A*, 1992, **93**, 91.
26 M.Ueshima and Y.Shimasaki, *Chem. Lett.*, 1992, 1345.
27 M. A. Aramendía, V. Borau, C. Jiménez, J. M. Marinas, A. Porras and F. J. Urbano, *Rapid Commun. Mass Spectrom.*, 1994, **8**, 599.
28 M. A. Aramendía, V. Borau, C. Jiménez, F. Lafont, J. M. Marinas, A. Porras and F. J. Urbano, *Rapid Commun. Mass Spectrom.*, 1995, **9**, 193.
29 D. D.Tomczak, J. L. Allen and K. R. Poeppelmeir, *J. Catal.*, 1994, **146**, 155.
30 R. Rudhan and A. I. Spiers, *J. Chem. Soc., Faraday Trans.*, 1997, **93**, 1445.
31 M. Hunger and T. Horvath, *J. Catal.*, 1997, **167**, 187.
32 S. Brunauer, P. H. Emmett and E. J. Teller, *J. Am. Chem. Soc.*, 1938, **60**, 309.
33 E. P. Barrett, L. S. Joyner and P. P. Halenda, *J. Am. Chem. Soc.*, 1951, **73**, 373.
34 F. M. Bautista, J. M. Campelo, A. García, D. Luna, J. M. Marinas and M. R. Urbano, *J. Mater. Chem.*, 1994, **4**, 311.
35 D. Mazza, M. Vallino and G. Busca, *J. Am. Ceram. Soc.*, 1992, **75**, 1929.
36 P. W. Kirlin, P. Auzins and J. E. Wertz, *J. Phys. Chem. Solids*, 1965, **26**, 1067.
37 T. Lopez, I. García-Cruz and R. Gómez, *Mater. Chem. Phys.*, 1994, **36**, 222.
38 R. Portillo, T. López, R. Gómez, A. Morales and O. Novaro, *Langmuir*, 1996, **12**, 40.
39 K. P. Peil, L. G. Galya and G.Marcelin, *J. Catal.*, 1989, **115**, 441.
40 D. Basset and H. W. Habgood, *J. Phys. Chem.*, 1960, **64**, 769.
41 H. Grisebach and J. B. Mofftat, *J. Catal.*, 1983, **80**, 350.
42 K. C. Waugh, M. Bowker, R. W. Petts, H. D. Vandervell and J. O'Malley, *Appl. Catal.*, 1986, **25**, 121.
43 E. Akiba, M. Soma, T. Onishi and K. Tamaru, *Z. Phys. Chem.*, 1980, **119**, 103.
44 M.Yamashita, F-Y. Dai, M.Suzuki, and Y. Saito, *Bull. Chem. Soc. Jpn.*, 1991, **64**, 628.

Paper 8/07536K